Environmental Earth Sciences (2021) 80:114
https://doi.org/10.1007/s12665-021-09395-y

ORIGINAL ARTICLE

Deformation and failure characteristics of composite coal mass

Yong Tao[1] · Li Zhenhua[3] · Cheng Zhiheng[2] · Zou Quanle[4] · Cao Jialin[2] · Huang Yanbo[2]

Received: 12 July 2020 / Accepted: 14 January 2021 / Published online: 2 February 2021
© The Author(s), under exclusive licence to Springer-Verlag GmbH, DE part of Springer Nature 2021

Abstract

This study analyzed stress characteristics and mechanical properties and compared the similarities and differences of composite coal mass with soft and hard coal mass in deformation and failure characteristics. Moreover, the mechanical properties and deformation and failure laws of the composite coal mass under unidirectional loading were investigated. The research results showed that for the composite coal mass, stress was distributed on each layer according to elastic modulus before reaching the peak pressure. However, after reaching the peak pressure, the soft layer first reached the strength limit, thus undergoing deformation and failure, and had softening effects on the overall bearing capacity of the composite coal mass. The degradation of the overall strength decreased and gradually increased with the rise of the height ratio of the soft layer. Under the same load, the degree of axial deformation of the composite coal sample reached the maximum. Deformation and failure of the composite coal mass could be divided into a stable stage, an accelerated stage and a failure stage. The failure of the soft layer induced damages to the upper and lower layers, while hard surrounding rock in the upper and lower layers constrained deformation and failure of the soft layer in the middle. Repeated adjustment of the stress field characterized the progressive failure of the composite coal mass.

Keywords Composite coal mass · Hard–soft interbed · Strength weakening · Dilatation · Progressive failure

Introduction

Composite coal seams are a kind of coal seams both containing soft and hard layers formed after movement of complex geological structure, which are commonly seen in thick coal seams. With the development of fully mechanized mining technologies (Wang 2014, 2015, 2019), especially the increase of mining height, heterogeneous coal walls with soft and hard interbeds are often seen in excavation sections of coal seams or the range of mining height, showing different layering characteristics. This makes coal walls prone to rib spalling and affects safe and efficient production in coal mines. Many scholars have conducted a lot of studies on mechanical mechanisms, failure mechanisms, control technologies and engineering practices of rib spalling of coal walls (Pang 2020; Si et al. 2019; Wang et al. 2016; Song et al. 2017; Yuan et al. 2013; Hua 2008; Yuan 2011). However, all of them are based on intact or homogeneous coal walls (coal mass) for analysis and the existing research results are not applicable to composite coal walls. Therefore, it is of great significance to study deformation and failure characteristics of the composite coal mass for preventing and controlling rib spalling of composite coal walls.

At present, there are a large number of studies on mechanical properties and deformation and failure laws of coal–rock composites in the world. Tien et al. (2000, 2006) carried out a series of researches on mechanical properties and deformation characteristics of layered rock mass and pointed out that the criteria of failure strength for homogeneous rock do not apply to the composite rock. Through a laboratory test, they investigated failure modes of the layered composite rock and put forward failure criteria thereof, and revealed

✉ Cheng Zhiheng
chengzhiheng21@vip.qq.com

✉ Zou Quanle
quanlezou2011@126.com

[1] School of Energy and Mining Engineering, China University of Mining and Technology (Beijing), Beijing 100083, China

[2] School of Safety Engineering, North China Institute of Science and Technology, Beijing 101601, China

[3] School of Energy Science and Engineering, Henan Polytechnic University, Jiaozuo 454000, Henan, China

[4] State Key Laboratory of Coal Mine Disaster Dynamics and Control, College of Resources and Environment Science, Chongqing University, Chongqing 400044, China

mechanisms and nature of anisotropy of mechanical properties of the layered rock. Based on the principle of energy equivalence, Zhao et al. (2015) studied overall stability of a coal–rock composite structure and established a model of equivalent mean energy and expression for stress states of the coal–rock composite. By combining with strength of the interface between coal and soft rock, they proposed the general compression–shear failure criteria of the model. Zuo et al. (2013) conducted uniaxial compression on a coal–rock composite and found that the energy carried by high-speed propagation of mixed cracks in coal can damage rock and the failure of the weak coal changes the overall failure of the coal–rock composite, thus reducing overall stability of the composite. It is considered that failure characteristics of the coal–rock composite are mainly controlled by weak part. Liu et al. (2009, 2011) regarded rock to be heterogeneous and divided it into a soft part containing pores and fractures and a hard part with matrix. Based on this, they established a stress–strain relationship and believed that the soft and hard parts meet Hooke's law through analysis. In the coal–rock composite, the coal layer is weaker. Chen et al. (Chen et al. 2019; Liu et al. 2015) held that strain and strain rate of coal are largely different from those of rock and that mechanical properties as well as deformation and failure behaviors of the composite are mainly affected by coal layers with low hardness. Strength characteristics of the composite mainly depend on coal strength rather than rock strength, let alone simply averaging. Heterogeneity of each layer in the coal–rock composite can result in difference of overall deformation and failure. Guo et al. (2018) performed a uniaxial compression test on the rock–coal–rock composites with different coal thicknesses and analyzed their mechanical behaviors. The overall peak strength and elastic modulus of the rock–coal–rock samples are between those of rock and coal and show a positive correlation with coal thickness. Failure mode is closely correlated with coal thickness.

According to the above research results, the coal–rock composite with quite different hardness of coal and rock are mainly studied, which have obvious deformation laws and failure characteristics. However, the composite coal mass whose hardness difference is low while has obvious influences is rarely studied. Due to different hardness coefficients, coal mass has distinct deformation laws and failure characteristics. Therefore, it is necessary to further investigate deformation and failure characteristics of the composite coal mass formed by combining soft and hard coal.

This study carried out a test on a composite coal sample formed by soft coal with hardness coefficient of about 1.5 and hard coal with hardness coefficient of about 3. Each layer with different hardnesses in the composite coal wall was simplified and the samples with same diameter and different height ratios were processed through a laboratory test. The processed different samples were superposed and combined into a composite coal sample for the uniaxial compression test based on the simplified hard–soft–hard model. This study analyzed stress characteristics and mechanical properties of different samples of the hard–soft–hard composites and discussed the failure modes. Studying mechanical properties and deformation and failure laws of the composite coal sample under unidirectional loading is conducive to further understanding failure mechanisms of the composite coal wall. By doing so, the research expects to provide references for studying failure of rib spalling and mechanical behaviors of the composite coal wall in a fully mechanized working face.

Overview of the test

Sample preparation

The coal samples used in the test were taken from a coal block with the dimensions of about 25 cm × 25 cm × 20 cm without obvious cracks from a relatively intact coal wall in fully mechanized working face with a large mining height. In the laboratory, by densely drilling cores along the direction of vertical bedding, the samples were processed into standard cylinder samples. Nonparallelism of the two ends of the sample was smaller than 0.05 mm and diameter deviation of the upper and lower ends was less than 0.3 mm. The processing precision met the test requirements. Through the uniaxial compression, the qualified coal samples were selected and processed into different types of ellipsoids. According to the simplified model, the samples were superposed and combined into a composite sample with the dimensions of Φ50 mm × 100 mm, that is, hard coal was distributed in upper and lower ends, while soft coal was sandwiched therebetween. The combination mode is displayed in Fig. 1.

Test scheme

The test was conducted using a RMT-301 mechanical test machine with the maximum axial loading of 1500 kN produced by North China Institute of Science and Technology, China. When measuring axial load, an extensometer was used with a horizontal range of 0–2.5 mm and a longitudinal range of 0–5 mm. The test accuracy of each test sensor was 0.5% of the current calibrated range at an equal ratio. A full digital computer was used for automatic control, with a variety of control modes including force, displacement and stroke control. Load and deformation were automatically collected during the test and displayed in real time. The test system is shown in Fig. 2.

The displacement-controlled loading at a rate of 0.001 mm/s was used in the test and continuous loading

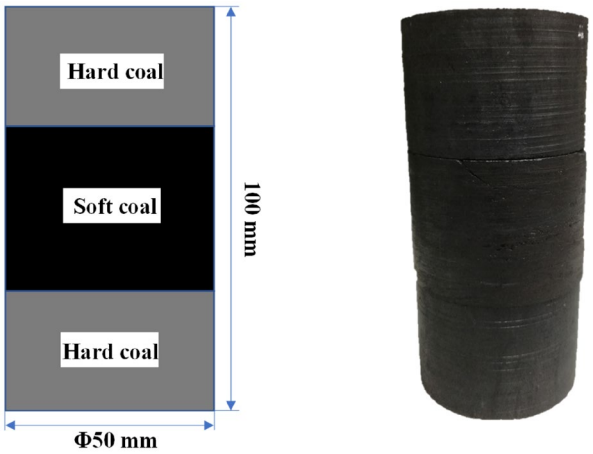

Fig. 1 Composite coal sample

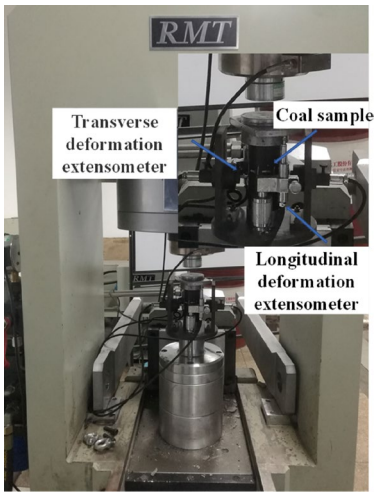

Fig. 2 RMT test system

was performed till the sample was completely damaged. Displacement sensors of 2.5 mm and 5 mm were separately used in the transverse and axial directions for measuring displacement of the sample and axial load of the sample was measured by utilizing a force sensor of 100 kN. Stress of the composite coal sample was the overall stress of the soft and hard coal composites, while axial strain was the sum of axial strains of the composites. An extensometer for radial deformation was installed in the soft coal mass, so radial strain was transverse strain of soft coal mass. The test design is illustrated in Fig. 3.

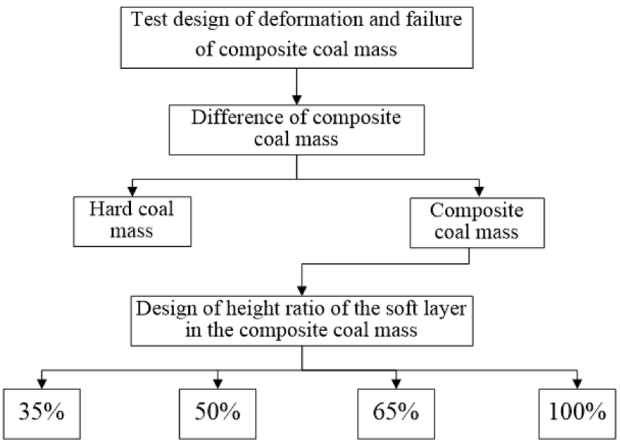

Fig. 3 Test design process

Results and discussions

Stress–strain relationship

Stress–strain curves of three coal samples (hard coal sample—YM, soft coal sample—RM, composite coal sample—FM) are shown in Fig. 4. Deformation of the composite coal samples can be divided into four stages (i.e., compaction, elastic, yield and failure stages) and is more obvious in the compaction stage compared with pure (hard or soft) samples, which mainly results from the presence of joint faces in the composite. The joint face, as a special crack, affects mechanical characteristics of the composite coal mass. After compaction of primary fractures and joint faces in the sample, deformation enters into the elastic stage, in which the sample can be approximately regarded as a continuous elastomer and stress–strain curve linearly rises. The composite coal sample shows a difference with pure hard or soft samples in the stage from yield to peak stress, especially when compared with hard coal mass: the composite coal sample does not reach the peak stress before producing large strain after entering into the yield stage. The stress–strain curve presents significant nonlinear changes and obvious yield characteristics. After load reaches the peak strength of the composite coal sample, internal cracks propagate and coalesce in a large scale, so that the sample finally loses bearing capacity. The analysis shows that the soft layer in the composite coal mass influences elastic–plastic relationship, with the addition of the soft layer in the composite coal body, the peak stress has an obvious downward trend. At the same time, its peak stress is lagging behind other coal samples, and the stress and strain show obvious nonlinear changes, and the heterogeneity of strength of the composite coal mass causes the soft layer with low strength to first gradually yield under stress.

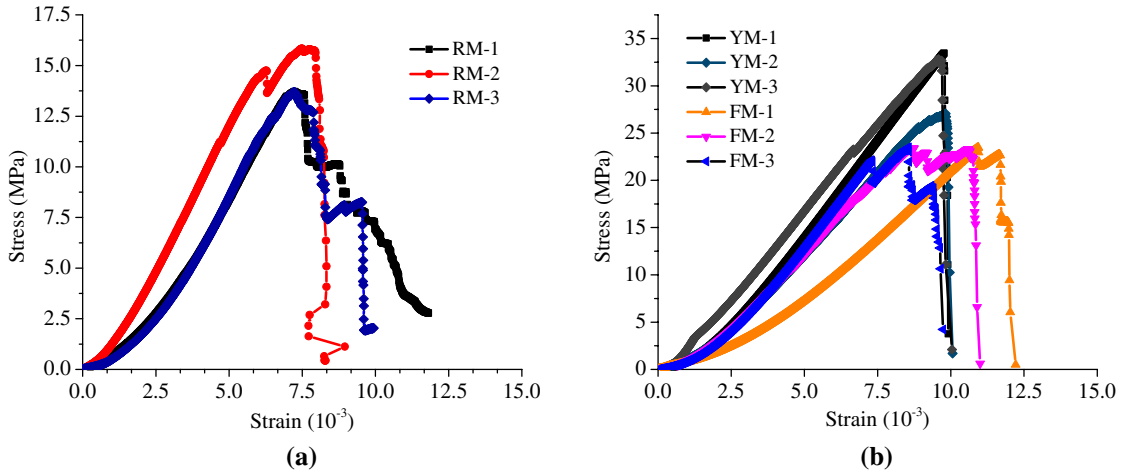

Fig. 4 Stress–strain curve. **a** Pure soft coal. **b** Pure hard coal and composite coal mass

Mean peak axial strains of the pure soft and hard coal samples separately are 0.0073 and 0.009, while that of the composite coal sample is 0.011. Peak axial strains of the FM-1 and FM-2 samples are obviously characterized, that is, under the same axial pressure, axial deformation of the composite coal sample is obviously greater than that of the pure soft and hard coal samples. The stress–strain curve of the composite coal sample obviously fluctuates at peak stress and presents significant nonlinear characteristics. Moreover, the sample is rapidly damaged after peak stress and finally loses bearing capacity, indicating that the composite coal sample is subjected to multiple progressive failure processes during loading. The composite coal sample shows rapid post-peak stress drops and obvious characteristics of brittle failure.

Change characteristics of strength

As shown in Fig. 4b, average compressive strengths of the pure hard coal sample and the composite coal sample are 31.11 and 23.45 MPa, respectively, so compressive strength of the composite coal sample is obviously smaller than that of the hard coal sample. The main reason is that lithologic heterogeneity greatly affects strength of the sample and the soft layer in the composite coal sample reduces overall bearing capacity, so that compressive strength decreases slightly. However, the strength is not weakened to a large extent, which is affected by the superposition effects of the composite to some extent. The influence mechanism is as follows: hard coal seams and soft coal seams alternate with each other, which improves the particle gradation, complements pore filling, and has obvious modification effects. The coal samples are intertwined, so the integrity of the coal samples is stronger. Macroscopically, the strength is higher, so that the strength of the composite coal sample becomes larger under the influence of the superposition effect.

The test was conducted according to design process in Fig. 3 and the strength of the composite coal mass was analyzed based on the changes of the height ratio of the soft layer. Uniaxial compressive strength is highly correlated with height ratio of the soft layer, and compressive strength nonlinearly decreases with the increase of the height ratio. The change trend is demonstrated in Fig. 5, in which height ratio of 0 represents the pure hard mass, while height ratio of 100% indicates the pure soft mass. The strength-weakening rate characterizes the influence degree of height ratio of the soft layer on strength of the composite coal mass and is expressed as $P_r = \left(P_n - P_{n+1}\right)/P_n$ (P_n and P_{n+1} represent the corresponding compressive strengths under different height ratios). When the height ratio of the soft layer changes from 0 to 35%, the strength weakening rate is the largest and

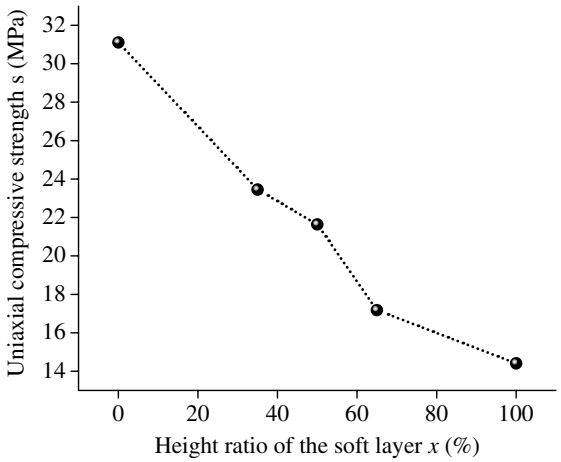

Fig. 5 Relationship between uniaxial compressive strength and height ratio of the soft layer

reaches 24.62%. As the height ratio varies from 35 to 50%, the strength-weakening rate is the smallest (7.72%). Therefore, this further indicates that the soft layer reduces bearing capacity of the composite coal mass. As the height ratio of the soft layer changes from 50 to 65%, the strength-weakening rate is 20.61%, following the maximum weakening rate. After the height of the soft layer exceeds the diameter of the sample, the strength weakening accelerates.

Analysis of deformation characteristics

For the composite coal mass, it is assumed that the external force is evenly transferred in the vertical direction and stresses of the hard and soft layers are equal. Then axial deformation is the sum of those of the soft and hard layers and measured transverse deformation is that of the soft layer, as shown in Fig. 6.

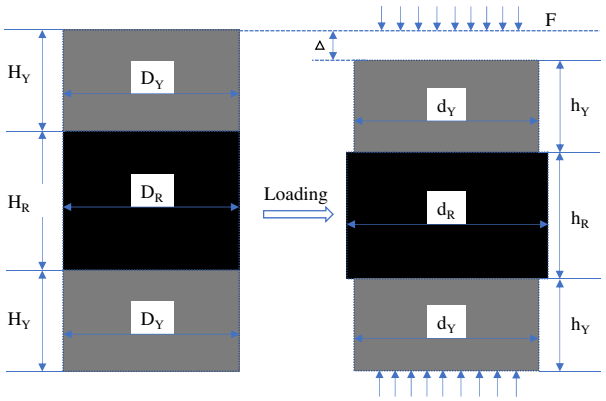

Fig. 6 Schematic diagram of deformation process of the composite coal mass under external force. F represents the external force, namely the force acted by the testing machine on the composite coal mass; H_Y and H_R indicate the heights of the hard layers in the upper and lower parts and the soft layer in the middle before loading, respectively; h_Y and h_R separately denote the heights of the hard layers in the upper and lower parts and the soft layer in the middle after loading; D_Y and D_R stand for the diameters of the hard layers in the upper and lower parts and the soft layer in the middle before loading, respectively; d_R and d_Y represent the diameters of the hard layers in the upper and lower parts and the soft layer in the middle after loading, respectively; Δ implies the displacement of the composite coal mass after loading

Under the external force F, it is assumed that the generalized stiffnesses of the composite coal mass, the upper hard layer, the soft layer and the lower hard layer are $E(\varepsilon)$, $E_1(\varepsilon)$, $E_2(\varepsilon)$ and $E_3(\varepsilon)$, respectively. Assuming that the total strain of the composite coal mass is ε, and strains of the above layers are ε_1, ε_2 and ε_3. The following formula is obtained:

$$F = E(\varepsilon)\varepsilon = E_1(\varepsilon)\varepsilon = E_2(\varepsilon)\varepsilon = E_3(\varepsilon)\varepsilon. \quad (1)$$

The generalized stiffness of the upper hard layer is same with that of the lower hard layer, namely $E_1(\varepsilon) = E_3(\varepsilon) = E_Y(\varepsilon)$ and for the soft layer, there is $E_2(\varepsilon) = E_R(\varepsilon)$, so

$$F = E(\varepsilon)\varepsilon = E_Y(\varepsilon)\varepsilon = E_R(\varepsilon)\varepsilon. \quad (2)$$

In accordance with stress–strain curves of the pure soft and hard coal in Fig. 4, compressive strength of the soft coal mass is greatly lower than that of the hard coal mass. The soft and hard layers do not reach the peak stress at the same time and their deformation is inconsistent, thus showing different mechanical characteristics.

In terms of mechanical differences of the soft and hard coal mass, under unidirectional loading, axial and radial strains change differently. Strain changes of the three types of coal samples in the test are shown in Fig. 7. It needs to point out that the radial strain of the composite coal mass measured is that of the soft layer in the middle.

Based on Fig. 7a and b, axial strains of the pure soft and hard coal gradually increase in the compaction stage. During the damaged from the elastic stage to peak, axial strain linearly changes, which is mainly related to displacement control used in the test. The increase rate of radial strain of the pure coal also gradually rises in the initial stage, which is relatively obvious. Failure of the pure hard coal linearly changes from the elastic stage to the peak. After entering the elastic

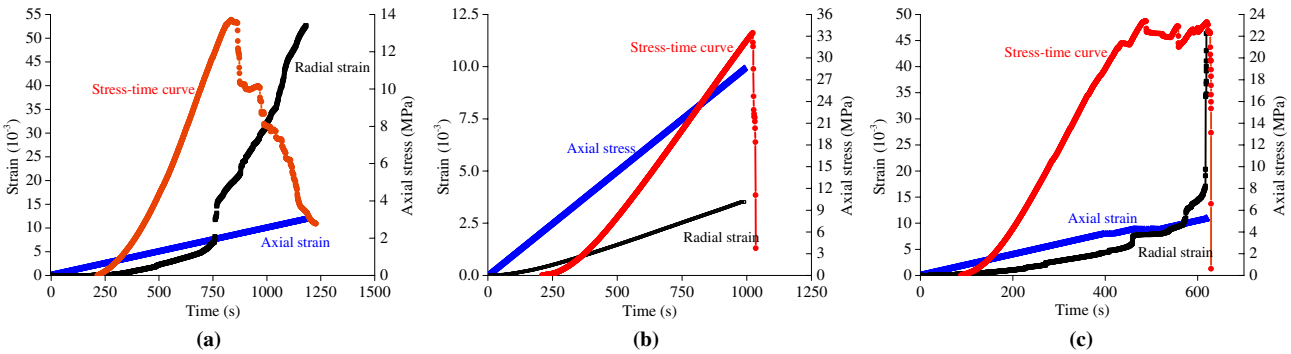

Fig. 7 Strain changes of different coal samples. **a** RM-1, **b** YM-1, and **c** FM-2

stage while before the yield stage, the pure soft coal shows that increase rate of radial strain gradually increases. After entering the yield stage while before the peak failure, there is a rapid increase in radial strain before and after yield and then the increase rate is slowing down but still fast. From the peak to the residual stage, increase rate of radial strain of the pure soft coal rises nonlinearly and fast. Through the above analysis, radial strains of the pure soft and hard coal differ largely and the soft coal mass shows more complex change rate and degree and more obvious dilatation compared with the hard coal mass.

Strain changes of the composite coal mass are presented in Fig. 7c. Axial and radial strains of the composite coal mass have different change laws with the pure soft and hard coal, which is mainly shown after the yield stage. On the whole, axial strain of the composite coal mass is larger than that of the pure soft coal, while radial strain is between those of the pure hard and soft coal. In the early stage of loading, increase rates of axial and radial strains both show a rising trend, while the increase rate of radial strain rises slowly. Axial strain is obviously greater than radial strain, which is similar with that of the pure soft and hard coal. After entering the yield stage while before the elastic stage, axial strain linearly changes, while increase rate of radial strain gradually reduces with very small amplitude, which approximately shows a linear change. As loading time increases, axial strain nonlinearly varies and fluctuates with small amplitude. The radial strain presents two abrupt rises in the increase rate, which gradually approaches to the axial strain curve. Moreover, radial strain exceeds axial strain at the second sharp rise of the increase rate and maintains rising at a high rate till obvious dilatation occurs in the peak failure stage.

Based on the above analysis, radial strain of the composite coal mass experiences three stages, i.e., stable deformation, accelerated deformation and obvious dilatation (although dilatation begins in the yield stage, it is unobvious in the early stage). In the stage of stable deformation, radial strain increases slowly and under the same stress, strain of the composite coal mass is smaller and increase rate is lower compared with the pure soft coal. This indicates that the hard layers in the composite coal mass greatly affect radial strain the soft layer in this stage, which corresponds to the compaction and elastic stages. In the stage of accelerated deformation, after entering the yield stage while before the peak failure, the radial strain exceeds the axial strain of the composite coal mass after two rapid growths of increase rate and the composite coal mass reaches the peak strength. However, radial strain exceeds axial strain after only one rapid growth of increase rate for the pure soft coal and the coal reaches the peak strength. The second sharp increase in increase rate of radial strain of the composite coal mass is similar to that of the pure soft coal. This implies that the soft layer is constrained by hard layers and the overall strength of the composite coal sample after continuously loading improves slightly compared with that of the pure soft coal. In the obvious dilatation stage, obvious dilatation is found at peak strength of the composite coal mass and dilatation rate is much larger than that of the pure soft coal. However, dilatation of the pure soft coal more continues more obviously from peak strength to the residual stage. In comparison with the pure soft coal, it is easy to find that the soft layer in the composite coal mass is largely influenced by the hard layers and radial strain of the soft layer is smaller than that of the pure soft coal, the rapid increase in radial strain of composite coal is similar to that of pure soft coal, indicating that the hard layers inhibit radial strain of the soft layer to some extent.

Elastic modulus

According to the test results, variation of elastic moduli of different types of coal mass is demonstrated in Fig. 8. When the height ratio of the soft layer in the composite coal mass is 35%, average elastic modulus is 3.388 GPa, which is 1.28 and 0.89 times those of the soft and hard coal mass. As the height ratios of the soft layer are 50% and 65%, average elastic moduli separately are 3.201 and 2.696 GPa, which separately reduce by 15.9%, 22.3%, 5.5% and 20.4% in comparison with hard coal mass and the case that the height ratio of the soft layer is 35%. Therefore, the soft layer weakens overall strength of the composite coal mass and decreases resistance to failure. With the increase of the height ratio of the soft layer, the elastic modulus shows a nonlinear downward trend in general and such trend accelerates after the height ratio exceeds the diameter. It needs to notice that elastic modulus of the composite coal sample is apparent elastic

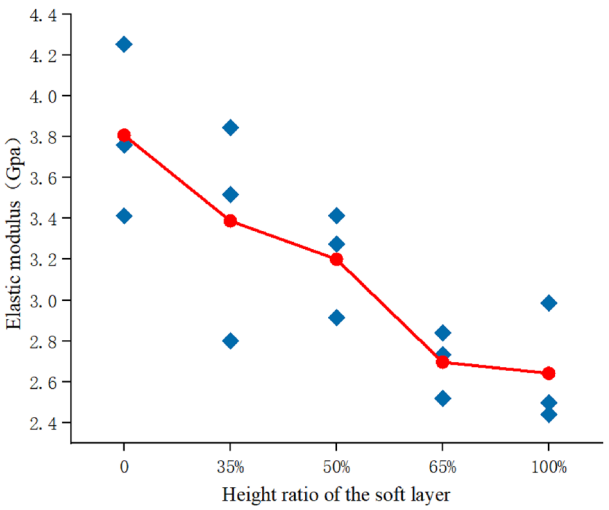

Fig. 8 Changes of elastic modulus of different height ratio of soft layer

modulus (Tan and Xian 1985), which is calculated according to the expression $\frac{1}{E_f} = \sum_{i=1}^{n} \frac{L_i}{E_i L}$. E_f, L_i, E_i and L represent the apparent elastic modulus of the composite coal mass, the height of the ith layer, the elastic modulus of the ith layer and the total height of the composite coal mass, respectively.

Analysis of failure characteristics

In the test, the pure soft and hard coal samples show two macro-failure modes, i.e., compression-shear failure and splitting failure. The pure soft coal is mainly dominated by compression-shear failure, while the pure hard coal mainly shows splitting failure, as displayed in Fig. 9a. The composite coal mass is different from pure soft and hard coal. Owing to failure strength of the upper and lower hard layers is higher than the strength of the soft layer in the middle, with the increase of load, cracks first appear in the middle soft layer. When reaching the peak load, rib spalling occurs in the soft layer and the upper layer presents shallow failure in the local region, while large vertical cracks are found in the lower layer. On the whole, the composite coal mass is mainly dominated by brittle failure, which first occurs in the soft layer in the middle. The intensified damage development and failure degree of the soft layer can induce damage and failure of the upper and lower hard layers to some extent. This is quite different from the failure of traditional homogeneous coal wall which mainly occurs in the middle and upper parts of the coal wall.

To better illustrate failure laws of the composite coal mass, the failure process is divided into three stages, namely stable development, progressive failure and failure stages in accordance with the test results.

The stable development stage starts from the early stage of loading to peak strength. In the early stage of loading, the joint faces, microcracks and pores in the composite coal mass are gradually closed under pressure and the soft and hard layers are gradually compacted. With the rise of stress, slope of the stress–strain curve gradually increases, indicating that closure of the microcracks gradually accelerates, and as the slope becomes smaller, the closure gradually slows down. Strain is assigned to each layer according to elastic modulus. Difference of elastic moduli of the layers results in different strains, which characterizes different deformation degrees of each layer. Deformation of the composite coal mass in this stage mainly occurs to the soft layer. During loading process of the composite coal mass, there is a crackling sound. At the macro-level, multiple cracks appear in the soft layer, as demonstrated in Fig. 10b.

Figure 10c intuitively shows characteristics of progressive failure of the composite coal mass. From the stress–strain curve, it can be seen that the pure soft coal smoothly changes from the pre-peak stage to the post-peak stage and the pure hard coal exhibits sudden drop of stress and rebound of elastic deformation. Different from this, the composite coal mass undergoes four times of stress drop and rebound and shows a similar rate, in which the maximum and minimum amplitudes are found in the second and third times, respectively. Moreover, there are three peaks and obvious characteristics of progressive failure. In this stage, the increase rate of radial strain of the composite coal mass accelerates, as marked by a red circle in Fig. 10a, indicating that deformation of the soft layer accelerates and dilatation is obvious. On the macro-level, fractures in the soft layer gradually develop and cracks coalesce to the upper and lower hard layers. Blocks are separated from the soft layer and small coal blocks are spalled in the shallow part at the end of the joint face in the upper hard layer, while vertical cracks appear on the surface of the lower hard layer. From the moment reaching the first peak strength (point A in Fig. 10c), stress rapidly decreases and strength reduces, while strain is small (strains corresponding to points A and B in Fig. 10c). Damage and fracture occurs in the soft layer, while multiple cracks appear

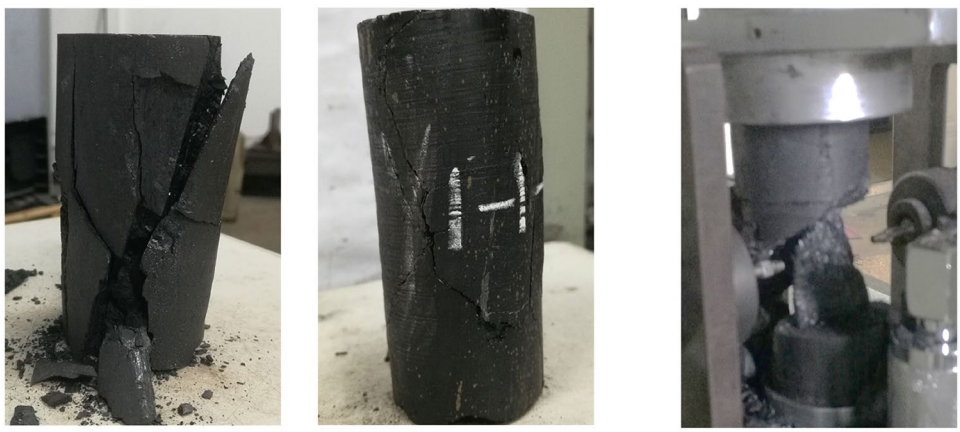

(a) (b)

Fig. 9 Failure characteristics of different types of coal mass. **a** Pure soft and hard coal. **b** Composite coal mass

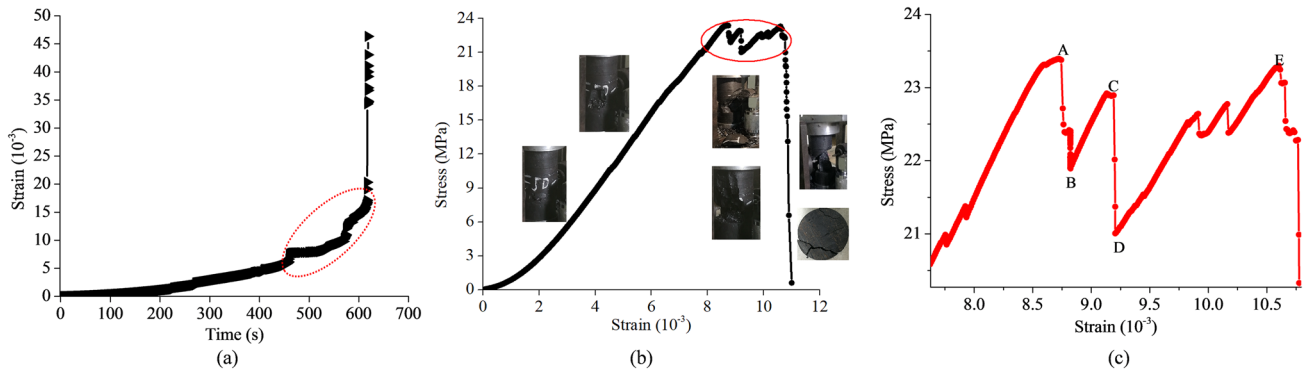

Fig. 10 Relationships of stress, strain and time of the composite coal mass. **a** Strain–time curve. **b** Stress–strain curve. **c** Stress–strain curve in the progressive failure

in the exterior macroscopically and the coal wall is spalled at the shallow part. With volume expansion and macro-failure of the soft layer, the upper and lower hard layers limit the deformation of the soft layer, which therefore is subjected to radial tensile stress, leading to changes of stress states of the soft and hard layers. Stress adjustment of the adjacent hard layers changes stress state of the composite coal mass, which shows rebound of stress and forms the second peak (point C in Fig. 10c). As pressure rises, damage and fracture further develops in the soft layer, accompanied with spalling of small coal blocks. During the failure process that strength rapidly decreases with the increase of strain, the decrease rate of strength is similar to the first peak and point D presents residual strength of the soft layer. After failure of the soft layer, deformation and failure occurs in the hard layers. Under the clamping action of the hard layers, the soft layer is found to have enhanced residual strength, which presents stress rebound again, and undamaged soft layer shares load with the hard layers. With the further increase of pressure, the soft and hard layers are damaged synchronously, and load is mainly undertaken by the hard coal layers. Serious macro-failure is found in the soft layer and the upper hard layer, while the lower hard layer only shows cracks while no macro-failure. With the increase of deformation, the lower hard layer is obviously compressed and stress rebounds transiently with small amplitude, which is lower than residual strength of the soft layer after failure. When reaching bearing limit of the composite coal mass, failure occurs to the whole composite and strain is significantly larger than the first two peak strengths. Moreover, deformation degree obviously increases. Stress at point E is the strength of the composite, namely peak strength of the composite coal mass. Therefore, the soft layer first reaches the bearing limit during stress loading and is constrained by the upper and lower hard layers during failure. Furthermore, the soft layer still has certain residual strength after failure and the hard layers are key layers bearing load to maintain the composite stable. When load is continuously applied, the soft layer is constantly damaged and the upper and lower hard layers are damaged. In this case, failure is mainly shown as the damage of hard coal mass.

After systematic failure, with the increase of strain, stress drops rapidly and strength decreases, so that the composite coal mass is damaged. The rapid reduction of stress after peak strength results from overall damage of the soft layer and hard surrounding rock. The composite is damaged on the whole and plastic deformation continuously develops. The composite coal mass (mainly the soft layer) reaches the strength to break and loosen and there is considerable volume dilatation. The strength of the composite coal mass finally is about zero.

Conclusions

This research studied mechanical properties of the composite coal mass and compared similarities and differences of deformation and failure characteristics of the composite coal mass with the soft and hard coal mass. The main conclusions are made as follows:

1. Under unidirectional loading, compared with the pure soft and hard coal, the stress–strain curve of the composite coal mass is more complex and shows nonlinear characteristics. The soft layer weakens bearing capacity of the composite coal mass and induces failure, with obvious weakening characteristics. The larger the height ratio of the soft layer is, the more obvious the weakening effects. The soft layer in the composite coal mass is confined by the hard layers, while the hard layers greatly affect radial strain of the soft layer, presenting distinct progressive failure characteristics.
2. Compared with homogeneous coal mass, the composite coal mass has obviously different failure characteristics.

The damage and failure of the soft layer results in the overall failure of the composite coal mass, while failure of the upper and lower hard layers dominates failure of the composite. The failure of the composite coal mass is slightly correlated with its elevation, while has a close relation with elevation where the soft layer is located.

3. In view of failure characteristics of the composite coal mass, in practices, the support or grouting of the soft layer in the composite coal wall should be strengthened to improve the strength, so as to avoid serious rib spalling induced by failure of the soft layer. At the same time, attention should be paid to the influence of the soft layer height ratio on the mechanical properties of the composite coal. With the increase of the height ratio of the soft layer, the uniaxial compressive capacity gradually decreases, indicating that the soft layer reduces the bearing capacity of the composite coal.

Acknowledgements This work is financially supported by National Natural Science Foundation of China (52074120 and 51774110), and the Fundamental Research Funds for the Central Universities (3142019005 and 3142017107), which are gratefully acknowledged.

References

Chen YL, Zuo JP, Liu DJ et al (2019) Deformation failure characteristics of coal-rock combined body under uniaxial compression: experimental and numerical investigations. Bull Eng Geol Env 78(5):3449–3464

Guo WY, Tan YL, Fu FH et al (2018) Mechanical behavior of rock-coal-rock specimens with different coal thicknesses. Geomechan Eng 15(4):1017–1027

Hua XZ, Xie GX (2008) Coal wall spalling mechanism and control technology of fully mechanized high cutting longwall mining face. Coal Sci Technol 36(9):1–3

Liu HH, Rutqvist J, Berryman JG (2009) On the relationship between stress and elastic strain for porous and fractured rock. Int J Rock Mech Min Sci 46(2):289–296

Liu HH, Rutqvist J, Birkholzer JT (2011) Constitutive relationships for elastic deformation of clay rock: data analysis. Rock Mechan Rock Eng 44(4):463–468

Liu J, Wang EY, Song DZ et al (2015) Effect of rock strength on failure mode and mechanical behavior of composite samples. Arab J Geosci 8(7):4527–4539

Pang YH, Wang GF, Yao QL (2020) Double-factor control method for calculating hydraulic support working resistance for longwall mining with large mining height. Arabian J Geosci13(6):252

Si L, Wang ZB, Liu XH et al (2019) Assessment of rib spalling hazard degree in mining face based on background subtraction algorithm and support vector machine. Curr Sci 116(12):2001–2012

Song G, Chugh Y, Wang J (2017) A numerical modelling study of longwall face stability in mining thick coal seams in China. Int J Mineral Eng 8(1):35–55

Tan X, Xian X (1985) Deformation and apparent elastic modulus of composite layered rock mass. Hebei Coal. 8(1):25–31

Tien Y, Tsao PF (2000) Preparation and mechanical properties of artificial transversely isotropic rock. Int J Rock Mechan Min Sci 37(6):1001–1002

Tien YM, Kuo MC, Juang CH (2006) An experimental investigation of the failure mechanism of simulated transversely isotropic rocks. Int J Rock Mech Min Sci 43(8):1163–1182

Wang J (2014) Development and prospect on fully mechanized mining in Chinese coal mines. Int J Coal Sci Technol 1(3):253–260

Wang J, Yu B, Kang H et al (2015) Key technologies and equipment for a fully mechanized top-coal caving operation with a large mining height at ultra-thick coal seams. Int J Coal Sci Technol 2(2):97–161

Wang J, Yang S, Kong D (2016) Failure mechanism and control technology of longwall coal face in large-cutting-height mining method. Int J Min Sci Technol 1(26):111–118

Wang K, Zhao T, Yetilmezsoy K et al (2019) Cutting-caving ratio optimization of fully mechanized caving mining with large mining height of extremely thick coal seam. Adv Civil Eng. ID:7246841. https://doi.org/10.1155/2019/7246841

Yuan Y, Tu SH, Wu Q et al (2011) Mechanics of rib spalling of high coal walls under fully-mechanized mining. Min Sci Technol (China) 21(1):129–133

Yuan Y, Tu SH, Zhang XG et al (2013) Mechanical and control technique of rib spalling disaster in fully-mechanized mining with large mining height in soft coal seam face. Disaster Adv 6(3):92–98

Zhao Z, Wang W, Wang L et al (2015) Compression-shear strength criterion of coal-rock combination model considering interface effect. Tunn Undergr Space Technol 47:193–199

Zuo J, Wang Z, Zhou H et al (2013) Failure behavior of a rock-coal-rock combined body with a weak coal interlayer. Int J Min Technol 23(6):907–912

Publisher's Note Springer Nature remains neutral with regard to jurisdictional claims in published maps and institutional affiliations.